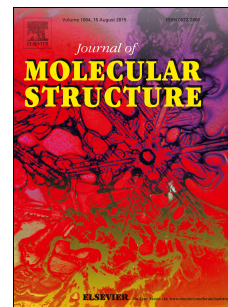


Accepted Manuscript

Open coordination sites-induced structural diversity of a new series of Cu(II) complexes with tridentate aroylhydrazone Schiff base

Guohong Xu, Beibei Tang, Leilei Gu, Pei Zhou, Hui Li



PII: S0022-2860(16)30480-X

DOI: [10.1016/j.molstruc.2016.05.034](https://doi.org/10.1016/j.molstruc.2016.05.034)

Reference: MOLSTR 22548

To appear in: *Journal of Molecular Structure*

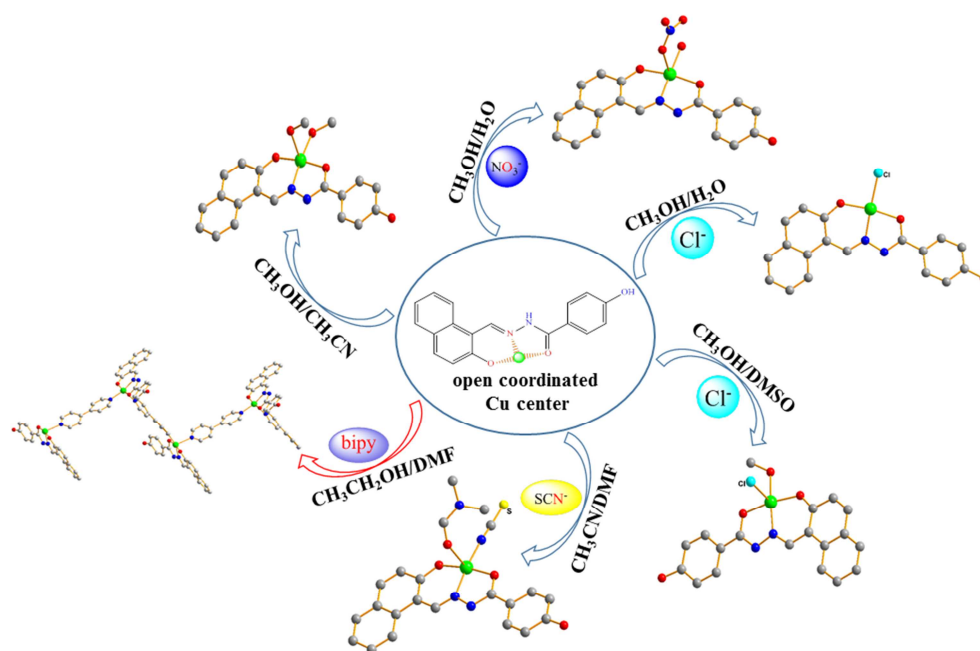
Received Date: 11 March 2016

Revised Date: 10 May 2016

Accepted Date: 11 May 2016

Please cite this article as: G. Xu, B. Tang, L. Gu, P. Zhou, H. Li, Open coordination sites-induced structural diversity of a new series of Cu(II) complexes with tridentate aroylhydrazone Schiff base, *Journal of Molecular Structure* (2016), doi: 10.1016/j.molstruc.2016.05.034.

This is a PDF file of an unedited manuscript that has been accepted for publication. As a service to our customers we are providing this early version of the manuscript. The manuscript will undergo copyediting, typesetting, and review of the resulting proof before it is published in its final form. Please note that during the production process errors may be discovered which could affect the content, and all legal disclaimers that apply to the journal pertain.



ACCEPTED MANUSCRIPT

Open coordination sites-induced structural diversity of a new series of Cu(II) complexes with tridentate aroylhydrazone Schiff base

Guohong Xu, Beibei Tang, Leilei Gu, Pei Zhou and Hui Li*

Key Laboratory of Cluster Science of Ministry of Education, School of Chemistry,
Beijing Institute of Technology, Beijing, 100081

Abstract

Six Cu(II) complexes containing the NO₂ donor tridentate asymmetrical aroylhydrazone ligand (E)-4-hydroxy-N'-((2-hydroxynaphthalen-1-yl)methylene)benzohydrazide (**HL**), namely, [Cu(L)Cl]·2H₂O (**1**), [Cu(L)(CH₃OH)₂]·NO₃ (**2**), [Cu(L)(NO₃)(H₂O)]·H₂O (**3**), [Cu(L)(CH₃OH)Cl]·CH₃OH (**4**), [Cu(L)(SCN)(DMF)]·DMF (**5**) and {[Cu(L)(4,4'-bipy)]ClO₄·4DMF}_n (**6**) have been synthesized and analyzed by x-ray single crystal diffraction. The structures of **1-6** are varied from zero-dimensional (0D) mononuclear complex to one-dimensional (1D) polymer based on the control of solvents, anions or auxiliary ligands, which can occupy the open coordination sites of Cu(II). Different hydrogen bonding interactions can also be observed in these complexes.

Keywords: Aroylhydrazone, Open coordination sites, Cu complex, Self-assembly, Hydrogen bonding, Supramolecular architecture

1. Introduction

Supramolecular metal-organic complexes have attracted enormous attentions owing to their interesting structures [1-14] and intriguing properties [15-25] for decades, which can be generated by coordination bond, hydrogen-bond, aromatic stacking, van der Waals interactions, and so on. Despite some advancement, the controllable synthesis of supramolecular complexes with pre-designed structures and desirable properties is a frontier and also a challenging task [26, 27]. Using appropriate organic ligands to design and create coordinatively opening sites of metal, which can be occupied by various ancillary moiety has been an effective approach to construct the diverse structures [28-36] and to tune the functional properties, such as fluorescence [28, 32, 35], magnetic [29-31], gas adsorptions [33, 36], and so on. Hence, to study the effect of the solvents, anions and auxiliary ligands on the self-assembly process based on multidentate ligands with

specific structural features is one of the crucial tasks.

We subsequently employed the aroylhydrazone Schiff base as ligand because of the following reasons: (i) this class of diprotic ligands typically act as tridentate, planar chelate ligands coordinating through the imine-N, carbonyl-O and phenolic-O atom, therefore, they have advantages in creating the open coordination sites of metal ion in complexes which can be occupied by auxiliary ligands, anions or solvents [37, 42-43], that is in favor of constructing the multi-nuclears or high-dimensional structures further. In addition, this kind of ligands with several oxygen donors and nitrogen donors can act as mono- and dianionic ligands due to their keto–enol tautomerism [37-42], therefore, which exhibit highly versatile coordination behaviour towards metal cations; (ii) aroylhydrazones constitute an interesting class of complexes with versatile structural features and fascinating potential application in advanced materials[44-48] and potential antimicrobial and antitumor activities [49-51].

Transition metal complexes derived from aroylhydrazone ligands can form diverse supramolecular networks as reported previously [41, 42, 44, 52]. Recently, one tetranuclear Zn(II) complex was synthesized by our group, which can be assembled into 3D diamondoid supramolecular framework through strong hydrogen bonding [44]. Thus, the wise modulation and tuning of the complementary sites responsible for hydrogen-bond formation have led to its application in supramolecular electronics [53], host-guest chemistry [54, 55], self-assembly of molecular capsules [56], and so forth.

In the present work, we have synthesized a NO₂ donor aroylhydrazone ligand through the condensation of 2-hydroxynaphthalene-1-carbaldehyde with 4-hydroxybenzohydrazide, namely, (E)-4-hydroxy-N'-((2-hydroxynaphthalen-1-yl)methylene)benzohydrazide. To understand the role of the solvents, anions and auxiliary ligands in the self-assembly process, we studied the crystal structure and supramolecular assembly of Cu(II) complexes with the asymmetrical aroylhydrazone ligand HL: [Cu(L)Cl]·1.5H₂O (1), [Cu(L)(CH₃OH)₂]·NO₃ (2), [Cu(L)(NO₃)(H₂O)]·H₂O (3), [Cu(L)(CH₃OH)Cl]·CH₃OH (4), [Cu(L)(SCN)(DMF)]·DMF (5) and {[Cu(L)(4,4'-bipy)]·ClO₄·4DMF}_n (6). Additionally, the complexes were characterized by means of FT-IR, UV-vis spectroscopy, elemental analysis and thermogravimetric analysis.

2. Experimental

2.1. Materials and measurements

All chemicals used for the synthesis were obtained from commercial sources and were used without further purification. Organic solvents used in this paper were of analytical purity. All reactions were carried out under atmospheric conditions. FT-IR spectrum is recorded in the Nicolet-360 FTIR spectrometer as KBr pellets in the 4000–400 cm^{-1} region, the resolution and the scan's numbers used to register the FTIR spectra are 4.000 and 32, respectively. Elemental analyses (C, H, N) were performed on a Flash EA1112 microanalyzer. The UV-vis absorption spectra were examined on a JASCO UV-1901 spectrophotometer in the wavelength range of 200–800 nm and the solvent used to register the UV-visible spectra is methanol. Thermo-gravimetric analyses (TGA) were carried out on a SEIKO TG/DTA 6200 thermal analyzer from room temperature to 800 °C at a ramp rate of 10 °C/min in a flowing 50 mL/min nitrogen atmosphere. ^1H NMR and ^{13}C NMR spectra was recorded on a Bruker ARX400 spectrometer (400 MHz) instrument in $\text{DMSO-}d^6$ with Me_4Si as the internal standard.

Caution! Perchlorate salts in presence of organic materials are potentially explosive and should be prepared in small amounts with appropriate precautions.

2.2. Preparation of the ligand HL

The 4-Hydroxybenzhydrazide (10 mmol, 1.522 g) and 2-hydroxy-1-naphthaldehyde (10 mmol, 1.720 g) were mixed in 40 mL ethanol in presence of 1 drop of concentrated hydrochloric acid. Then, the mixture was refluxed for 8 hours (80 °C) with vigorous stirring and subsequently cooled to room temperature. The resulting yellow precipitate was collected by vacuum filtration. A yellow powder was obtained after being washed with ethanol and dried in air (Scheme S1). Yield: 83.4%. Anal. Calcd for $\text{C}_{18}\text{H}_{14}\text{N}_2\text{O}_3$: C, 70.58; H, 4.61; N, 9.15. Found: C, 70.62; H, 4.68; N, 9.17. Selected IR (KBr pellet, cm^{-1}): $\nu(\text{O-H})$ 3433; $\nu(\text{N-H})$ 3289, 3167; $\nu(\text{C=O})$ 1634; $\nu(\text{C=N})^+$ amide 1606-1537. ^1H NMR (400 MHz, $\text{DMSO-}d^6$): δ (ppm) 12.91 (s, 1H), 12.03 (s, 1H), 10.25 (s, 1H), 9.48 (s, 1H), 8.19 (d, 1H, $J = 7.2$), 7.90 (m, 4H), 7.62 (s, 1H), 7.42 (s, 1H), 7.24 (d, 1H, $J = 8.3$), 6.92 (d, 2H, $J = 6.9$). ^{13}C NMR (100 MHz, $\text{DMSO-}d^6$) δ (ppm) 162.62, 161.50, 158.34, 146.35, 132.94, 132.06, 130.15, 129.46, 128.27, 128.18, 123.97, 123.55, 120.93, 119.42, 115.72, 109.06.

2.3. Preparation of complex $[\text{Cu}(\text{L})\text{Cl}] \cdot 1.5\text{H}_2\text{O}$ (1)

The water solution (4 mL) of $\text{CuCl}_2 \cdot 2\text{H}_2\text{O}$ (9 mg, 0.05 mmol) was placed at the bottom of tube, and then carefully added the methanol solution (12 mL) of **HL** (15 mg, 0.05 mmol) to allow slow liquid-to-liquid diffusion. Green needle single crystal suitable for X-ray analysis were produced by in two days. Yield: 65%. Anal. Calcd for $\text{CuC}_{18}\text{H}_{16}\text{N}_2\text{O}_{4.5}\text{Cl}$: C, 50.12; H, 3.74; N, 6.49. Found: C, 50.20; H, 3.53; N, 6.50. Selected IR (KBr pellet, cm^{-1}): $\nu(\text{O-H})/\nu(\text{N-H})$ 3123; $\nu(\text{C=O})$ 1658; $\nu(\text{C=N})^+$ amide 1617–1537.

2.4. Preparation of complex $[\text{Cu}(\text{L})(\text{CH}_3\text{OH})_2] \cdot \text{NO}_3$ (2)

The solution of $\text{Cu}(\text{NO}_3)_2 \cdot 2\text{H}_2\text{O}$ (12 mg, 0.05 mmol) in 2 mL methanol was added by methanol / acetonitrile (V : V = 6 : 1) solution (7 mL) of **HL** (15 mg, 0.05 mmol) with continuous stirring for 15 min. The result solution was then filtered and left at room temperature to give a deep green solution. Green cubic single crystal suitable for X-ray analysis were produced by slow evaporation of the mother liquor for seven days. Yield: 78%. Anal. Calcd for $\text{CuC}_{20}\text{H}_{21}\text{N}_3\text{O}_8$: C, 48.53; H, 4.28; N, 8.49. Found: C, 48.51; H, 4.26; N, 8.50. Selected IR (KBr pellet, cm^{-1}): $\nu(\text{O-H})$ 3185; $\nu(\text{N-H})$ 3035; $\nu(\text{C=O})$ 1600; $\nu(\text{C=N})^+$ amide 1576–1511.

2.5. Preparation of complex $[\text{Cu}(\text{L})(\text{NO}_3)(\text{H}_2\text{O})] \cdot \text{H}_2\text{O}$ (3)

The solution of $\text{Cu}(\text{NO}_3)_2 \cdot 2\text{H}_2\text{O}$ (12 mg, 0.05 mmol) in 2 mL water was added by solution of **HL** (15 mg, 0.05 mmol) in 6 mL methanol. The reaction solution was filtrated after stirring with 15 minutes. Suitable Green prism single crystals for X-ray diffraction were obtained by slow evaporation of the mother liquor for three days. Yield: 68%. Anal. Calcd for $\text{CuC}_{18}\text{H}_{17}\text{N}_3\text{O}_8$: C, 46.30; H, 3.67; N, 9.00; Found: C, 46.28; H, 3.69; N, 8.98. Selected IR (KBr pellet, cm^{-1}): $\nu(\text{O-H})$ 3183; $\nu(\text{N-H})$ 3020; $\nu(\text{C=O})$ 1621; $\nu(\text{C=N})^+$ amide 1576–1512.

2.6. Preparation of complex $[\text{Cu}(\text{L})(\text{CH}_3\text{OH})\text{Cl}] \cdot \text{CH}_3\text{OH}$ (4)

The methanol solution of **HL** (26 mg, 0.10 mmol) was mixed with the methanol solution of CuCl (10 mg, 0.10 mmol) with stirring, and then 10 mL DMSO was added to the mixture solution. The mixture was stirred with ca. 40 min. at room temperature to give a deep green solution. Suitable green single crystals for the structure determination were obtained by slow evaporation of the mother liquor for two days. Yield: 80%. Anal. Calcd for $\text{CuC}_{20}\text{H}_{21}\text{N}_2\text{O}_5\text{Cl}$: C, 51.29; H, 4.52; N, 5.98. Found: C, 51.25; H, 4.50; N, 5.97. Selected IR (KBr pellet, cm^{-1}): $\nu(\text{O-H})/\nu(\text{N-H})$ 3157; $\nu(\text{C=O})$ 1654; $\nu(\text{C=N})^+$ amide 1615–1551.

2.7. Preparation of complex [Cu(L)(SCN)(DMF)]·DMF (5)

The MeCN solution (5 ml) of Cu(ClO₄)₂·6H₂O (19mg, 0.05 mmol) was slowly added the MeCN/DMF (V : V = 5 : 1) solution of the **HL** (15mg, 0.05 mmol) and KSCN (10mg, 0.1 mmol). The dark green reaction mixture was stirred for one hour and filtrated. The resulting filtrate was left at room temperature one day during which green parallelogram single crystals were obtained. Calcd for CuC₂₅H₂₇N₅O₅S: C, 52.39; H, 4.75; N, 12.22. Found: C, 52.36; H, 4.765; N, 12.19. Selected IR (KBr pellet, cm⁻¹): ν(O-H)/ν(N-H) 3037; ν(SCN) 2107; ν(C=O) 1646; ν(C=N)⁺ amide 1618–1539.

2.8. Preparation of complex {[Cu(L)(4,4'-bipy)]·ClO₄·4DMF}_n (6)

The ethanolic solution (3 mL) of Cu(ClO₄)₂·6H₂O (37 mg, 0.1 mmol) was slowly added the ethanolic solution (5 mL) of the **HL** (30 mg, 0.1 mmol). After ca. 15 min, the ethanolic solution solution (2 mL) of 4, 4'-bipyridine (20 mg, 0.1 mmol) was added, and then the precipitate appeared. DMF was added dropwise to the mixture solution until the precipitate dissolved. Suitable green parallelogram single crystals for X-ray diffraction were obtained by slow evaporation of the mother liquor for three days. Calcd for CuC₃₄H₃₅N₆O₉Cl: C, 52.99; H, 4.58; N, 10.90. Found: C, 52.95; H, 4.57; N, 10.91. Selected IR (KBr pellet, cm⁻¹): ν(O-H)/ν(N-H) 3021; ν(C=O) 1676; ν(C=N)⁺ amide 1616–1520.

2.9. X-ray crystal structure determinations

Diffraction intensities for six complexes were collected on a Rigaku RAXIS-RAPID CCD diffractometer equipped with a graphite- monochromatic MoK α radiation ($\lambda = 0.71073\text{\AA}$) using an ω scan mode at $296 \pm 2\text{K}$ (complex 2), 153.15 (complex 1, 3-6). Diffraction intensity data were collected in the θ range of $3.06\text{-}29.13^\circ$ for complex 1, $1.78\text{-}24.99^\circ$ for complex 2, $3.07\text{-}27.48^\circ$ for complex 3, $2.32\text{-}25.00^\circ$ for complex 4, $3.03\text{-}24.99^\circ$ for complex 5, and $2.21\text{-}29.13^\circ$ for complex 6. The collected data were reduced using the SAINT program [57], and empirical absorption corrections were performed using the SADABS program [57]. Six structures were solved by direct methods [58] and refined using full-matrix least square techniques on F^2 [59] with the program SHELXL-97 [57]. All nonhydrogen atomic positions were located in difference Fourier maps and

refined anisotropically. Some of hydrogen atoms were placed in their geometrically generated positions and other hydrogen atoms were located from the different Fourier map and refined isotropically. Crystallographic data are given in Table 1. Selected bond distances and angles are given in Table 2.

Table 1 Crystal data and structure refinement for complex **1-6**.

	1	2	3	4
Formula	CuC ₁₈ H ₁₆ N ₂ O _{4.5} Cl	CuC ₂₀ H ₂₁ N ₃ O ₈	CuC ₁₈ H ₁₇ N ₃ O ₈	CuC ₂₀ H ₂₁ N ₂ O ₅ Cl
fw	431.32	494.94	466.90	468.38
T (K)	153(2)	296(2)	153(2)	153(2)
Cryst. Svst.	monoclinic	monoclinic	monoclinic	triclinic
Space group	P2/n	P2 ₁ /c	C2/c	P-1
<i>a</i> (Å)	15.536(3)	9.5931(17)	22.441(4)	7.4373(15)
<i>b</i> (Å)	6.9299(14)	9.5735(17)	9.2875(19)	10.923(2)
<i>c</i> (Å)	16.753(3)	22.945(4)	19.111(4)	12.885(3)
α (°)	90	90	90	96.54(3)
β (°)	111.69(3)	92.029(5)	109.28(3)	103.06(3)
γ (°)	90	90	90	104.42(3)
<i>V</i> (Å ³)	1675.9(6)	2106.0(6)	3759.7(13)	971.4(3)
<i>Z</i>	4	4	8	2
ρ calcd. (mg·m ⁻³)	1.705	1.561	1.650	1.601
F(000)	876	1020	1912	482
θ rang. (°)	3.06-29.13	1.78-24.99	3.07-27.48	2.32-25.00
μ (mm ⁻¹)	1.494	1.091	1.216	1.298
λ (Å)	0.71073	0.71073	0.71073	0.71073
R (int)	0.0395	0.0401	0.0444	0.0262
FinalR1,wR2[I>2 σ (I)]	0.0387,0.0840	0.0512, 0.1004	0.0467, 0.1096	0.0382, 0.0813
R1, wR2(all data)	0.0500,0.0889	0.0715, 0.1083	0.1096, 0.1193	0.0415, 0.0847
Peak and hole (e Å ⁻³)	0.735,-0.559	0.461,-0.458	0.510, -0.335	0.820, -0.263
	5	6		
Formula	CuC ₂₅ H ₂₇ N ₅ O ₅ S	CuC ₃₄ H ₃₅ N ₆ O ₉ Cl		
fw	573.12	770.67		
T (K)	153(2)	153(2)		
Cryst. Svst.	monoclinic	monoclinic		
Space group	P2 ₁ /c	P2 ₁ /n		
<i>a</i> (Å)	14.275(3)	10.248(2)		
<i>b</i> (Å)	7.6358(15)	18.178(4)		
<i>c</i> (Å)	23.608(5)	18.605(4)		
α (°)	90	90		
β (°)	91.66(3)	98.63(3)		
γ (°)	90	90		
<i>V</i> (Å ³)	2572.2(9)	3426.5(12)		
<i>Z</i>	4	4		
ρ calcd. (mg·m ⁻³)	1.480	1.494		
F(000)	1188	1596		
θ rang. (°)	3.03- 24.99	2.21 -29.13		
μ (mm ⁻¹)	0.976	1.298		
λ (Å)	0.71073	0.71073		
R (int)	0.0883	0.0505		
FinalR1,wR2[I>2 σ (I)]	0.0614, 0.1434	0.0557, 0.1058		
R1, wR2(all data)	0.0948, 0.1565	0.0768, 0.1148		
Peak and hole(e Å ⁻³)	1.183, -0.907	0.389, -0.357		

Table 2 Selected bond distances (Å) and bond angles (°) for complexes **1-6**.

1			
O(2)-C(7)	1.264(3)	O(3)-Cu(1)-N(2)	90.26(7)
N(1)-C(7)	1.341(3)	O(3)-Cu(1)-O(2)	171.68(7)
Cu(1)-O(3)	1.9009(16)	N(2)-Cu(1)-O(2)	81.47(7)
Cu(1)-N(2)	1.9239(19)	O(3)-Cu(1)-Cl(1)	92.59(6)
Cu(1)-O(2)	1.9601(16)	N(2)-Cu(1)-Cl(1)	176.40(6)
Cu(1)-Cl(1)	2.2350(9)	O(2)-Cu(1)-Cl(1)	95.71(6)
2			
O(2)-C(12)	1.268(5)	N(1)-Cu(1)-O(4)	173.42(13)
N(2)-C(12)	1.329(5)	O(1)-Cu(1)-O(2)	172.82(13)
Cu(1)-O(3)	2.447(3)	N(1)-Cu(1)-O(2)	82.25(12)
Cu(1)-O(1)	1.875(2)	O(4)-Cu(1)-O(2)	93.69(12)
Cu(1)-N(1)	1.906(3)	O(1)-Cu(1)-O(3)	93.29(11)
Cu(1)-O(4)	1.944(3)	N(1)-Cu(1)-O(3)	92.69(12)
Cu(1)-O(2)	1.950(2)	O(4)-Cu(1)-O(3)	92.59(14)
N(1)-Cu(1)-O(1)	92.24(12)	O(2)-Cu(1)-O(3)	91.56(11)
O(1)-Cu(1)-O(4)	91.37(13)		
3			
O(2)-C(12)	1.257(3)	O(1)-Cu(1)-O(3)	92.73(8)
N(2)-C(12)	1.355(3)	N(1)-Cu(1)-O(2)	81.96(8)
Cu(1)-N(1)	1.903(2)	O(1)-Cu(1)-O(2)	171.14(8)
Cu(1)-O(1)	1.9190(18)	O(3)-Cu(1)-O(2)	95.03(8)
Cu(1)-O(3)	1.935(2)	N(1)-Cu(1)-O(5)	93.59(8)
Cu(1)-O(2)	1.9923(19)	O(1)-Cu(1)-O(5)	91.77(8)
Cu(1)-O(5)	2.471(2)	O(3)-Cu(1)-O(5)	84.04(8)
N(1)-Cu(1)-O(1)	90.46(9)	O(2)-Cu(1)-O(5)	93.27(8)
N(1)-Cu(1)-O(3)	176.08(9)		
4			
O(2)-C(7)	1.269(3)	O(3)-Cu(1)-O(4)	88.81(7)
N(1)-C(7)	1.340(3)	N(2)-Cu(1)-O(4)	167.16(8)
Cu(1)-O(3)	1.8891(18)	O(3)-Cu(1)-O(2)	168.36(7)
Cu(1)-N(2)	1.911(2)	N(2)-Cu(1)-O(2)	81.76(8)
Cu(1)-O(4)	1.9461(18)	O(4)-Cu(1)-O(2)	95.07(7)
Cu(1)-O(2)	1.9752(17)	Cl(2)-Cu(1)-O(3)	96.73(6)
Cu(1)-Cl(2)	2.7070(11)	Cl(2)-Cu(1)-N(2)	101.55(7)
O(3)-Cu(1)-N(2)	92.04(8)	Cl(2)-Cu(1)-O(4)	91.07(6)
		Cl(2)-Cu(1)-O(2)	94.17(6)

5			
O(2)-C(15)	1.261(5)	N(2)-Cu(1)-O(3)	90.58(14)
N(1)-C(15)	1.351(5)	N(3)-Cu(1)-O(3)	93.57(15)
Cu(1)-O(3)	1.913(3)	N(2)-Cu(1)-N(3)	173.61(16)
Cu(1)-N(2)	1.923(4)	O(3)-Cu(1)-O(2)	171.55(12)
Cu(1)-N(3)	1.927(4)	N(2)-Cu(1)-O(2)	81.64(14)
Cu(1)-O(2)	2.007(3)	N(3)-Cu(1)-O(2)	93.92(15)
6			
O(1)-C(7)	1.269(3)	O(2)-Cu(1)-O(1)	167.01(7)
N(1)-C(7)	1.340(3)	N(2)-Cu(1)-O(1)	80.83(8)
Cu(1)-O(2)	1.9057(18)	N(4)-Cu(1)-O(2)	93.27(8)
Cu(1)-N(2)	1.944(2)	N(2)-Cu(1)-N(4)	161.49(8)
Cu(1)-O(1)	1.9822(18)	N(4)-Cu(1)-O(1)	92.31(8)
Cu(1)-N(4)	2.008(2)	N(3)-Cu(1)-O(2)	95.63(8)
Cu(1)-N(3)	2.282(2)	N(2)-Cu(1)-N(3)	94.07(8)
N(2)-Cu(1)-O(2)	90.27(8)	N(3)-Cu(1)-O(1)	94.43(7)
		N(4)-Cu(1)-N(3)	103.63(8)

3. Results and discussion

3.1. Synthesis of the complexes

With different Cu salts (Cl^- , NO_3^- , ClO_4^-) and solvents, four different kinds of mononuclear Cu complexes 1-4 are obtained. By the employment of the distinct secondary ligands SCN^- and 4,4'-bipy, mononuclear Cu complex 5 and 1D coordination complex 6 were constructed.

The phenolic hydroxyl and naphthalene ring introduced in the ligand HL have enhanced the intermolecular interaction but weaken the bridging role, which prompted the different mononuclear structure of complexes 1-5, thus addition of the auxiliary ligand (4,4'-bipy) is advantageous to construct one-dimensional (1D) chain (complex 6). Based upon the synthesis conditions, the Cu(II) is tetra-coordinated in complex 1 and penta-coordinated in 2-6, it is noteworthy that the aroylhydrazone ligand in the six complexes are exclusively monoanionic and in the keto form to coordinate to Cu ion, which can be verified from C=O and C-NH bond lengths of the amide unit. Amide unit bond lengths for aroylhydrazones are in the ranges of 1.241–1.280 Å (C–O), 1.336–1.386 Å (C–N), and 1.296–1.314 Å (C–O), 1.294–1.310 Å (C–N) in the keto and enol form, respectively [39-42, 60].

3.2. Crystal structural description

3.2.1. $[\text{Cu}(\text{L})\text{Cl}] \cdot 2\text{H}_2\text{O}$ (**1**)

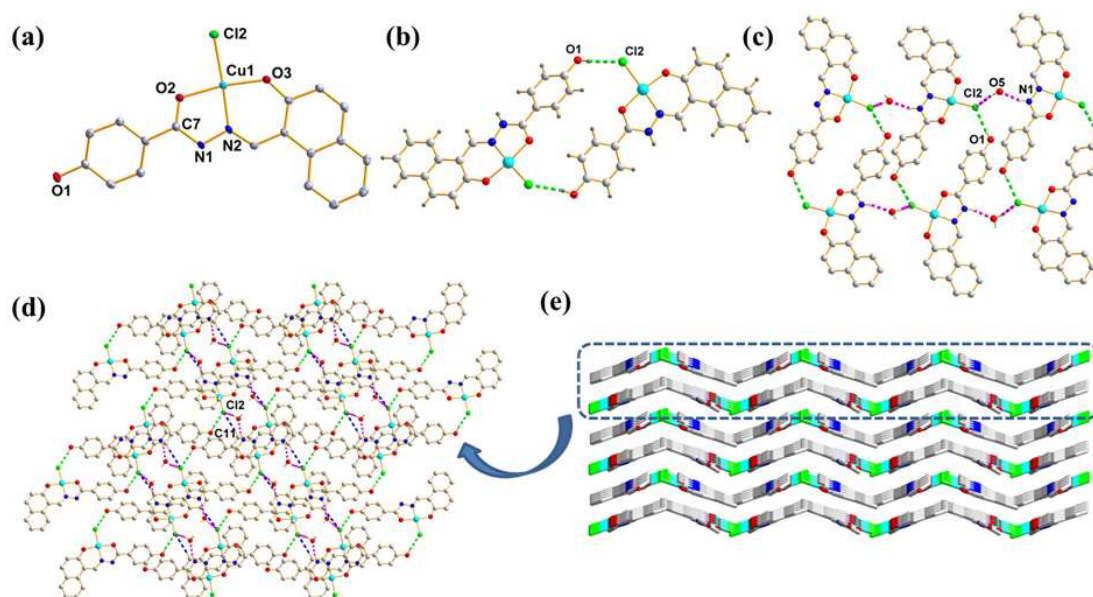


Fig. 1. (a) View of coordination environments of Cu and ligand in **1**. Uncoordinated solvent molecule (or anion) and hydrogen atoms are omitted for clarity. (b) Dimeric unit formed by intermolecular O–H...Cl interaction in **1** (green dashed line). (c) Packing diagram of **1** showing the zigzag chain formation through N–H...O and O–H...Cl hydrogen-bonding interactions (pink dashed line). (d) Perspective view of the stacking array of **1** showing the formation of a 2D layer through C–H...Cl intermolecular interactions (blue dashed line). (e) The 3D structure of **1** by van der Waals interaction. Hydrogen atoms not involved in hydrogen-bonding interactions are omitted for clarity.

Single-crystal X-ray analysis on complex **1** shows that it is mononuclear and the copper(II) is tetra-coordinated. The asymmetric unit of the complex **1** is depicted in Fig. 1a. The arylhydrazone ligand is coordinated as a mono-negative tridentate chelating agent via the imine-N, carbonyl-O and phenoxo-O atom which make one five-membered and one six-membered chelate rings. The fourth coordination position is occupied by the chloride ligand. The Cu(1)–O [1.9009(16) Å and 1.9601(16) Å] and Cu(1)–N[1.9239(19)Å] bond distances are comparable with corresponding values reported in other similar copper(II) complexes [37, 42]. The deviations of the four donor atoms O2, N2, O3, and C11 from their least-squares mean plane through them are 0.026(3), 0.029(6), -0.025(5), and 0.022(2) Å, respectively. The Cu atom deviates from the mean plane by 0.013(9) Å. The dihedral angle between the mean planes of the five-membered chelate ring and the six-membered one is 1.5°.

The uncoordinated oxygen atom of terminal -OH group donates a hydrogen bond to the chloride atom of the adjacent asymmetric unit, resulting in a dimer (Fig. 1b). The crystal packing of complex **1** shows several intermolecular H-bonds such as O–H...Cl, C–H...Cl and N–H...O as

shown. The oxygen atom (O5) of the uncoordinated water molecule acts as a single hydrogen bonding donor to chloride atom (Cl2) of one neighbor (O5–H5B...Cl2A) and a single hydrogen bonding acceptor from amido group nitrogen atom (N1) of the other neighbor (N1–H1A...O5). Through these hydrogen bond interactions a 1D chain is generated (Fig. 1c). Apart from these interactions, C–H...Cl interaction was observed between the chloride atom and the naphthalene ring. These supramolecular interactions extend 1D chain to a 2D supramolecular layer (Fig. 1d). The supramolecular layers further stabilize the crystal structure via the van der Waals interaction (Fig. 1e).

Table 3 Distances (Å) and angles (°) of hydrogen bonds for 1-6.

D–H...A	d(H...A)	d(D...A)	∠D–H...A
1			
O1–H1...Cl2 #1	2.343	3.147	166.91
O5–H100...Cl2#2	2.482	3.225	168.14
N1–H1A...O5	1.891	2.726	163.43
C11–H11...Cl2	2.938	3.852	167.7
2			
O4–H22...O3#3	1.886	2.686	172.00
O5–H5...O6#4	1.966	2.717	151.82
O3–H23...O6#5	1.985	2.733	169.26
N2–H21...O7#6	2.022	2.873	170.41
3			
N2–H2...O5#7	2.047	2.788	143.77
O4–H4...O1#8	1.887	2.705	175.93
O3–H30...O8#9	1.784	2.608	173.75
O8–H8B...O7#10	1.989	2.833	171.91
O8–H8A...O4#11	1.998	2.843	172.14
4			
N1–H1A...Cl2#12	2.420	3.211	153.27
O1–H1...Cl2#13	2.340	3.138	164.41
O4–H4A...O5	1.856	2.628	150.14
O5–H5A...Cl2#14	2.410	3.185	157.82
5			
N1–H100...O4#15	2.027	2.837	156.68
C25A–H25A...O1	2.468	3.402	168.5
O1–H1...O5#16	1.821	2.628	167.78
6			
C4–H4A...N3	2.713	3.643	179.1
O3–H3...O8#17	1.811	2.629	174.76

N1–H35···O6#18	2.037	2.859	159.67
N1–H35···C11#18	2.873	3.690	159.39

Symmetry transformations used to generate equivalent atoms: #1: $-x+3/2, y, -z+1/2$. #2: $x+1/2, -y, z+1/2$. #3: $-x, -y, -z$. #4: $x, -y+1/2, z-1/2$. #5: $x, y, z-1$. #6: $-x+1, -y+1, -z+1$. #7: $-x, -y, -z+1$. #8: $x, -y, z-1/2$. #9: $-x+1/2, -y+1/2, -z+1$. #10: $x, -y, z-1/2$. #11: $x, y+1, z$. #12: $-x+1, -y+1, -z+1$. #13: $x, y-1, z$. #14: $x-1, y, z$. #15: $-x, -y+1, -z$. #16: $x, y, z-1$. #17: $x+1, y, z$. #18: $x+1/2, -y+1/2, z-1/2$.

3.2.2. [Cu(L)(CH₃OH)₂·NO₃ (2), [Cu(L)(NO₃)(H₂O)]·H₂O (3) and [Cu(L)(CH₃OH)Cl]·CH₃OH (4)

Under different synthetic conditions, the complexes 2, 3 and 4 which are all mononuclear and penta-coordinated have been obtained. In them, the obvious difference is that the remaining sites of Cu(II) in complex 2 are occupied by two solvent atoms to form coordinated cation while in the others which are occupied by one solvent atom and one anion to form coordination complexes. The bond lengths in complex 2-4 are within the expected range for Cu(II) complexes with aroylhydrazone ligands [41, 42].

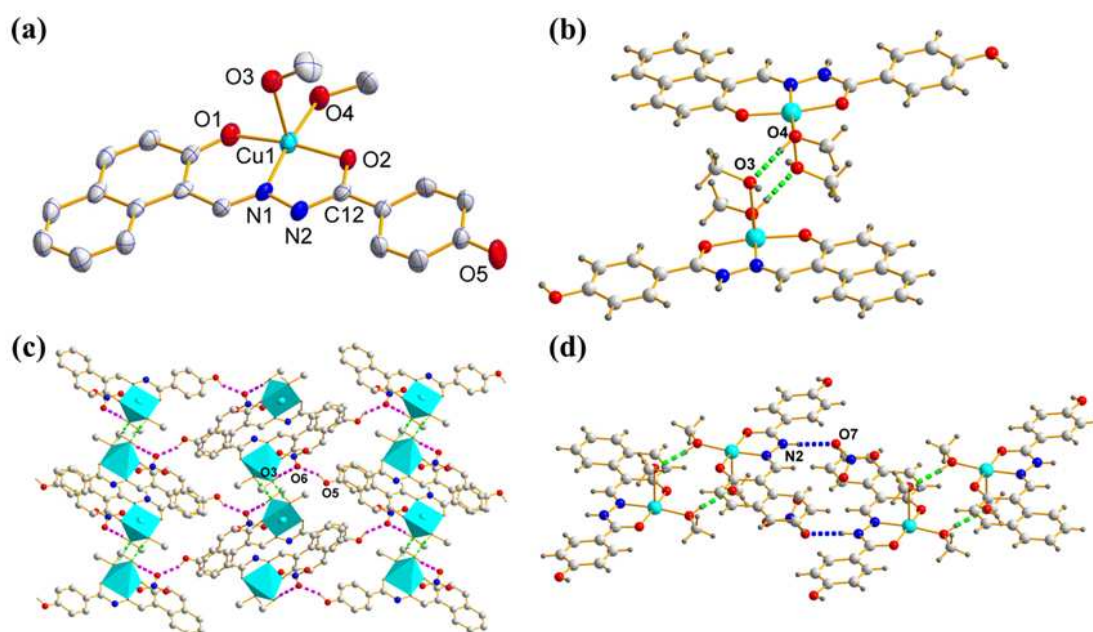


Fig. 2. (a) View of coordination environments of Cu and ligand in **2**. Uncoordinated solvent molecule (or anion) and hydrogen atoms are omitted for clarity. (b) Dimeric unit formed by intermolecular O–H···O interaction in **2** (green dashed line). (c) Packing diagram of **2** showing the 2D H-bonded network (pink dashed line). Hydrogen atoms not involved in H-bonding are omitted for clarity. (d) The 3D H-bonding of **2** (blue dashed line).

Single-crystal X-ray analysis on complex 2 (Fig. 2a) shows that the asymmetric unit contains a complex cation and a nitrate anion. Therefore, the complex 2 is monocationic and is stabilized by a nitrate counteranion in the lattice. The ligand is mono-negative and coordinates in a tridentate mode via the O, N, O-donor atoms. The remaining sites in the penta-coordinate arrangement are occupied by two methanol oxygen atoms (O3 and O4). The coordination sphere is best described

as square pyramid by the τ value (0.01) defined by Addison et al. ($\tau = 0$ for an ideal square pyramid, and 1 for an ideal trigonal bipyramid) [61].

In this description, the methanol-O3 atom occupies an axial position. The long distance of the Cu1–O3 bond with 2.447(3) Å shows weak bonding of the methanol to the central copper atom due to the Jahn-Teller effect [62]. The entire aroylhydrazone ligand is nearly planar with a small twist and the dihedral angle between the benzene and naphthalene rings is 7°. This overall planarity is consistent with the observation that each of the five- and six-membered chelate rings is planar having r.m.s. deviations of 0.006(6) and 0.028(5) Å, respectively.

As X-ray study, we conclude significant hydrogen bonding interactions are present in the crystal structures of **2**. The -OH hydrogen atoms of both coordinated methanol molecules of complex **2** are involved in hydrogen bonding (Table 3). The methanol molecule oxygen atom (O4) of one asymmetric unit act as hydrogen bond donors to the methanol molecule oxygen atom (O3) of an adjacent unit, forming a dimer via one pair of O4–H22...O3 hydrogen bonds (Fig. 2b). Although the nitrate anions are not coordinated to the Cu(II) centres in complex **2**, they are involved in a hydrogen bonding. Nitrate anions regard as bridges connecting neighboring Cu(II) dimeric units to form the 2D net-like open framework structure as shown in Fig. 2c. The nitrate oxygen atom (O6) acts as a double hydrogen bonding acceptor from methanol oxygen atom (O3) and uncoordinated phenolic oxygen atom (O5) of the adjacent binuclear entities. (O5–H5...O6 and O3–H23...O6). Meanwhile, nitrate oxygen atom (O7) acts as a single hydrogen bonding acceptor from uncoordinated amido nitrogen atom (N2) of another neighboring molecules, resulting in 3D structure (Fig. 1d and Fig. S4).

Compared with the complex **2**, a little different coordination environment is observed in **3**. The key difference is oxygen atom of nitrate anion occupies the axial position in **3** (Fig. 3a). The NO₄ coordination donor set defines a square-pyramidal coordination arrangement ($\tau = 0.08$). The five- and six-membered chelate rings are planar (r.m.s. deviations = 0.004(2) and 0.013(2) Å, respectively) but a slightly greater twist in the overall aroylhydrazone ligand [dihedral angle between the benzene rings = 9.7°] is observed in **3** compared with that in **2**.

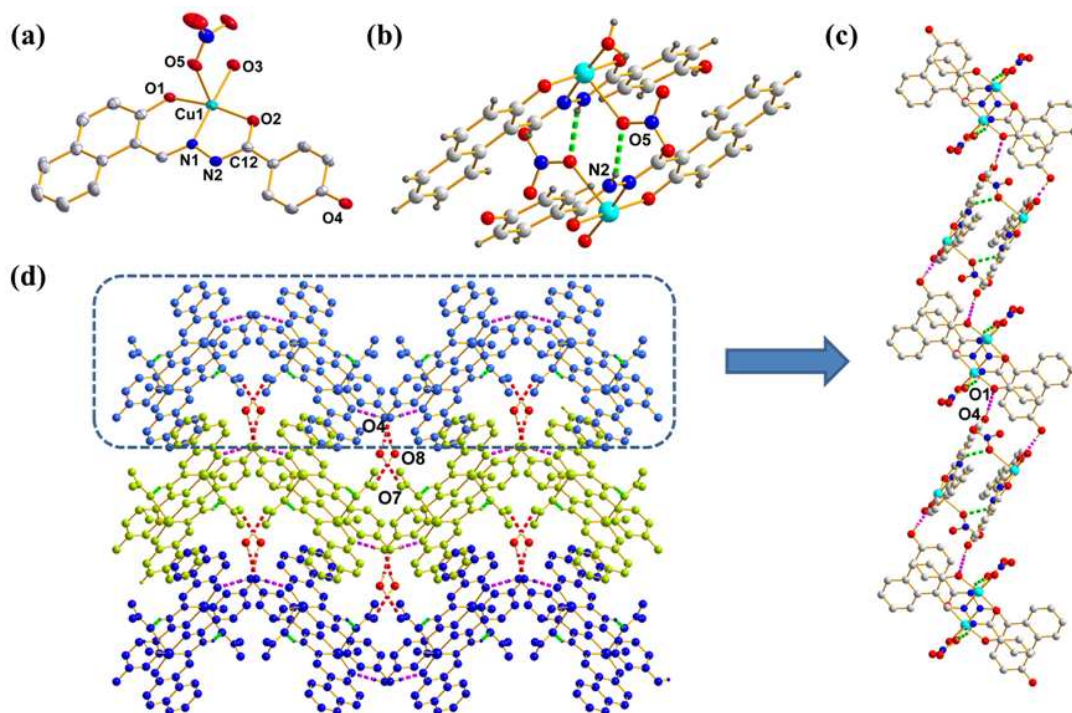


Fig. 3. (a) View of coordination environments of Cu and ligand in **3**. Uncoordinated solvent molecule (or anion) and hydrogen atoms are omitted for clarity. (b) Dimeric unit formed by intermolecular N–H···O interaction in **3** (green dashed line). (c) Packing diagram of **3** showing the zigzag chain formation through O–H···O hydrogen-bonding interactions (pink dashed line). (d) Perspective view of the stacking array of **3** showing the formation of a 2D layer through O–H···O intermolecular interactions (red dashed line). Hydrogen atoms not involved in hydrogen-bonding interactions are omitted for clarity.

The hydrogen atom H2 of the amido (–NH–) group forms a strong hydrogen bond with the oxygen atom O5 of the coordinated nitrate anion of a centrosymmetrically related unit to form a hydrogen bonded dimeric entity (Fig. 3b). Additionally, each molecule of **3** interacts with two neighbors to form 1D zigzag chain by intermolecular hydrogen-bonding interactions between the uncoordinated oxygen atoms of terminal –OH groups in ligand and coordinated –OH groups (Fig. 3c). The 1D chains are further connected via O8–H8B···O7 and O8–H8A···O4 interactions from two adjacent chains to form a 2D layer-like structure (Fig. 3d). In addition, the presence of interlayer hydrogen bonds (O3–H30···O8) leads to the formation of a 3D supramolecular network (Fig. S5 and Fig. S6), which contributes to the additional stability of the structure.

In the process of synthesizing complex **2** and **3**, only the solvent is different. Distinct structural differences between **2** and **3** indicated that the solvent remarkably affect the structure of the resulting complexes. Although the structures of **2** and **3** apparently look very similar, a comparison of the structures and dimensions in Table 1, clearly show that the arrangement of the donor atoms around the metal is very different.

By changing the metal salt and solvents, obtained the mononuclear complex **4**. The copper(II) in **4** is NO_3Cl penta-coordinated and chloride atom occupies the axial position (Fig. 4a). The coordination polyhedron around the Cu(II) ion could be best described as square pyramidal, which is reflected by the τ value(0.02). The basal plane is built by two oxygen atom and one nitrogen atom from the aroylhydrazone ligand and one methanol molecular. The base is nearly coplanar, with the largest deviation from the mean plane is 0.019(3) Å for N2. As is commonly observed in square pyramidal complexes, the Cu (II) ion is displaced by 0.194(7) Å from the basal plane towards the apical chloride. In addition, there is an appreciable Jahn-Teller effect highlighted by an axial Cu1–Cl2 distance (2.7070(11) Å) significantly longer than that observed for equatorial Cu1–Cl1 distance in **1** (2.2350(9) Å) and shorter than that in dichlorido-bridged Cu(II) complex [43].

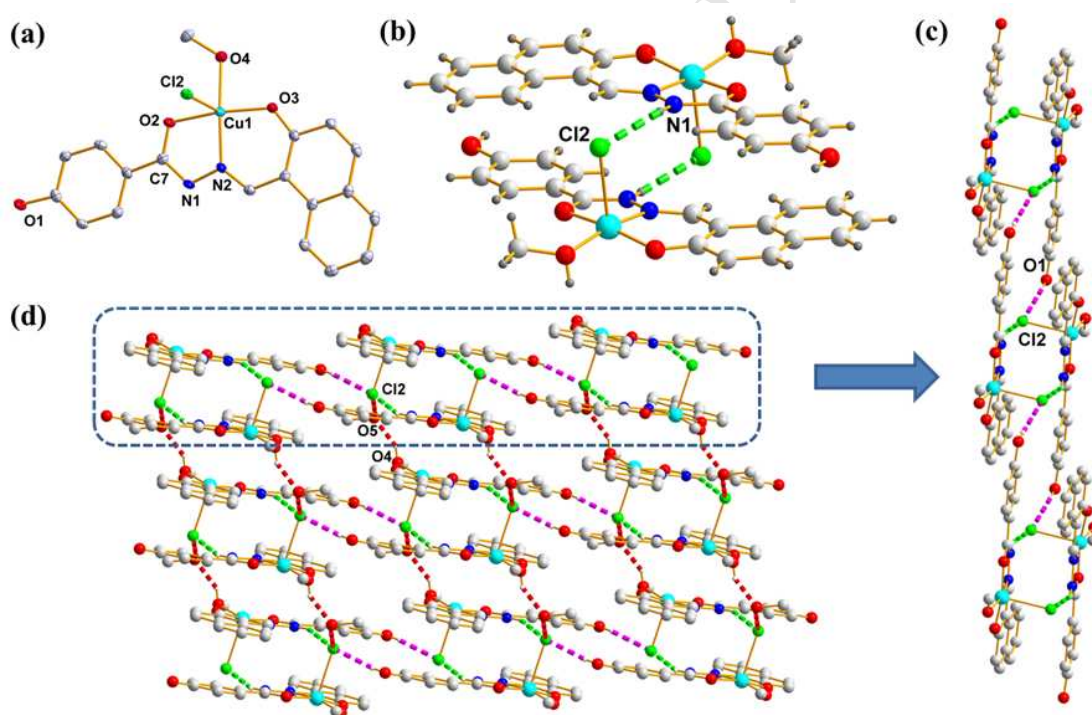


Fig. 4. (a) View of coordination environments of Cu and ligand in **4**. Uncoordinated solvent molecule (or anion) and hydrogen atoms are omitted for clarity. (b) Dimeric unit formed by intermolecular N–H...Cl interaction in **4** (green dashed line). (c) Packing diagram of **4** showing the 1D chain formation through O–H...Cl and O–H...O hydrogen-bonding interactions (pink dashed line). (d) Perspective view of the stacking array of **4** showing the formation of a 2D layer through O–H...Cl intermolecular interactions (red dashed line). Hydrogen atoms not involved in hydrogen-bonding interactions are omitted for clarity.

In **4**, the amido group nitrogen atom (N1) of one asymmetric unit act as hydrogen bond donors to chloride atom (Cl2) of an adjacent unit, forming a dimer, and the two aroylhydrazone ligands in the dimer are nearly parallel (Fig. 4b). There exist intermolecular hydrogen bonds between the

uncoordinated oxygen atom of terminal -OH group and the chloride atom, O1–H1...Cl2, through which a 1D supramolecular chain is generated (Fig. 4c). The oxygen atom (O5) of the uncoordinated methanol molecular acts as a single hydrogen bonding donor to chloride atom (Cl2) of one neighbor and a single hydrogen bonding acceptor from coordinated methanol molecular oxygen atom (O4) of another neighbor, resulting in a 2D layer structure (Fig. 4d). The adjacent layers are extended to a 3D supramolecular architecture by van der Waals interaction (Fig. S7).

3.2.3. [Cu(L)(SCN)(DMF)]·DMF (**5**) and {[Cu(L)(4,4'-bipy)]·ClO₄·4DMF}_n (**6**)

As mentioned above, the aroylhydrazone ligand HL has advantages in generating the open coordination sites of copper ion in complexes which can be occupied by anions, solvents or auxiliary ligands to construct new structure entities which can be self-assembled into higher order architectures. To study this academic point of view, besides tuning the anions and solvents in the complexes **1-4**, we further employed the thiocyanate and 4,4'-bipyridine as auxiliary ligand in the complex **5** and **6**, respectively.

By adding potassium thiocyanate as the auxiliary ligand, obtained the new complex **5**. Single-crystal X-ray studies revealed that the complex **5** crystallises in the monoclinic space group $P2_1/c$. A view of the molecular structure of **5** is presented in Fig. 5. The complex **5** consists of one mono-negative Schiff base L⁻, one N-terminal SCN⁻ anions and two solvent DMF molecules. The Cu(II) ion displays square-pyramid coordination ($\tau=0.03$) with three ligating atoms O2, O3, and N2 from the same ligand, one N3 atom from one terminal SCN⁻ anion and one O4 atom from DMF molecule. The thiocyanate group acts as a monodentate ligand and is linear within the experimental error [$N3-C17-S2 = 178.1(5)^\circ$]. The Cu1–N3–C17 angle of $170.9(4)^\circ$ is usual for terminally coordinated N-bonded thiocyanate [63]. The deviations of the four donor atoms O2, O3, N2, and N3 from their least-squares mean plane through them are $-0.008(9)$, $-0.008(6)$, $0.009(4)$, and $0.008(1)$ Å. The Cu atom deviates from the mean plane by $0.070(5)$ Å. The dihedral angles between the two planes [N2–Cu1–O3 and O2–Cu1–N3] is 6.1° . The two diagonal O3–Cu1–O2 and N2–Cu1–N3 angles of the complex [$171.55(12)$ and $173.61(16)$] are less than 180° .

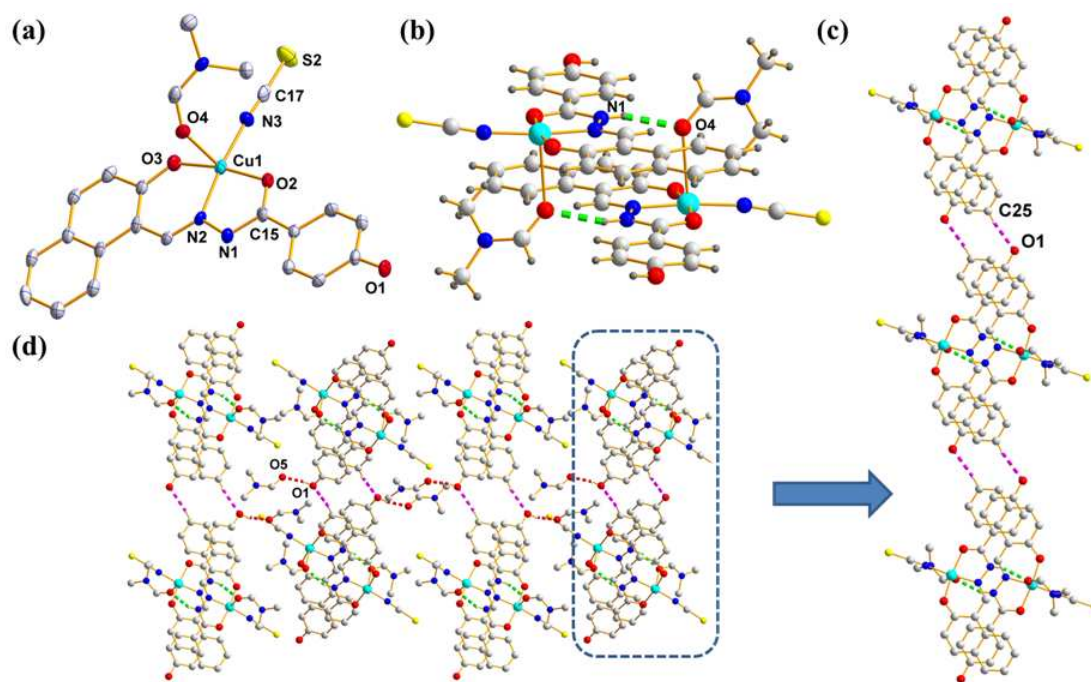


Fig. 5. (a) View of coordination environments of Cu and ligand in **5**. Uncoordinated solvent molecule and hydrogen atoms are omitted for clarity. (b) Dimeric unit formed by intermolecular N–H···O interaction in **5** (green dashed line). (c) Packing diagram of **5** showing the 1D chain formation through C–H···O hydrogen-bonding interactions indicated (pink dashed line). (d) Perspective view of the stacking array of **5** showing the formation of a 2D layer through O–H···O intermolecular interactions (red dashed line). Hydrogen atoms not involved in hydrogen-bonding interactions are omitted for clarity.

Firstly, the amido group nitrogen atom (N3) of one asymmetric unit act as hydrogen bond donors to the DMF molecule oxygen atom (O4) of an adjacent unit, forming a dimer via one pair of N1–H100···O4 hydrogen bonds (Fig. 5b). Secondly, the dimmers form a 1D supramolecular chain by non-conventional hydrogen bonds among benzene group and uncoordinated -OH group (C25A–H25A···O1) (Fig. 5c). The uncoordinated DMF molecular is involved in constructing hydrogen bonding. The hydrogen bond O–H···O joins neighbouring 1D chains together to form a 2D supramolecular layer (Fig. 5d). The DMF molecular oxygen atom (O5) acts as a hydrogen bonding acceptor from uncoordinated phenolic oxygen atom (O1) of the adjacent chains. Finally, the van der Waals force connects adjacent 2D supramolecular layers and results in the formation of the 3D supramolecular network (Fig. S8).

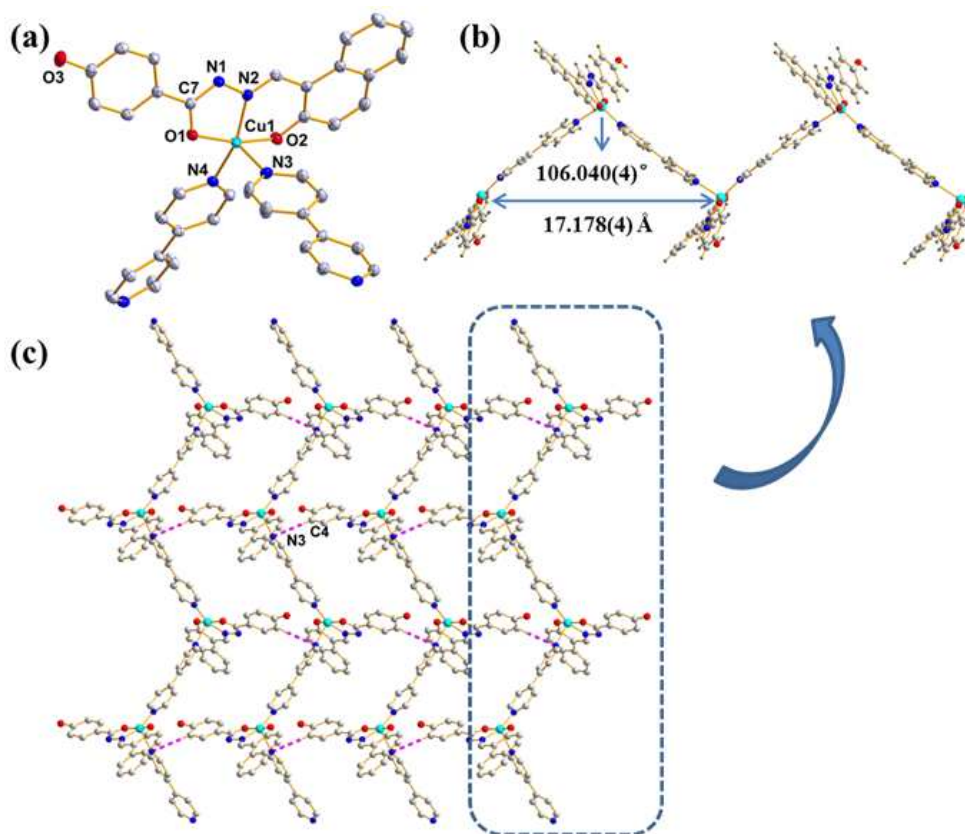


Fig. 6. (a) Crystal structure of **6** with atom numbering scheme. (b) The infinite 1D zigzag chain structure of **6**. (c) The 2D structure of **6**. Hydrogen atoms not involved in hydrogen-bonding interactions are omitted for clarity.

By adding 4,4'-bipyridine as the auxiliary ligand, with its bridging role, a 1-D zigzag chain structure of Cu complex **6** was built. X-ray crystallographic analysis revealed that the complex **6** crystallizes in the monoclinic space group of $P2_1/n$ and the asymmetric unit contains one Cu(II) center, one ligand anion L^- , one 4,4'-bipyridine, one ClO_4^- anion and four free DMF molecules. The coordination environment around the Cu (II) center in **6** is presented in Fig. 6 with atom numbering scheme. Each Cu (II) atom is penta-coordinated by O1, O2 and N2 atoms from one tridentate ligand and two N atoms (N3 and N4) from two 4, 4'-bipyridine molecules to form a CuN_3O_2 coordination environment. The Cu (II) atom adopts an approximately square pyramidal geometry, which is reflected by the τ value (0.092) defined by Addison et al.

The basal plane of the square pyramid is defined by O1, O2, N2 and N4 atoms, with the bond distances ranging from 1.9057(18) to 2.008(2) Å and bond angles ranging from 80.83(8) to 167.01(7)°. The Cu(II) atom lies approximately in the equatorial position with a deviation (0.2432 Å) from the basal plane. The axial coordination site is occupied by N3 atom from another 4, 4'-bipyridine molecule with Cu-N3 of 2.282(2) Å. Thus, the coordination geometry of the Cu (II) atom in **6** can be regarded as a distorted square pyramid. On the other hand, the ligand L^- anion,

also employed as a tridentate chelating agent, coordinated to the Cu (II) atom with its ONO donor atoms in meridional fashion. And the bridging 4,4'-bipyridine molecules also link the Cu(L) units to form a 1D zigzag chain structure (Fig. 6b). In this zigzag chain, the chain length $d = 17.178(4)$ Å, and the bending angle $\theta = 106.040(4)^\circ$. The two pyridyl rings of 4,4'-bipyridine are twisted at an angle of 17.280° with respect to one another, and the corresponding Cu \cdots Cu intermetallic distance separated by 4,4'-bipyridine is 11.3777 Å.

The adjacent 1D chains were further assembled by hydrogen bonds to produce an infinite 2D network. The resulting 2D supramolecular structure is held together via non-conventional H-bonding C–H \cdots N (Fig. 6c). The C4 atom of benzene ring and N3 atom of amido group are involved in the formation of C–H \cdots N hydrogen bonds. Moreover, the uncoordinated N atom of amido group and perchlorate are interlinked through N–H \cdots O and N–H \cdots Cl hydrogen bonds, ultimately leading to a 3D supramolecular framework (Fig. S9 and Fig. S10). Therefore, 1D chain entities are self-assembled through the H-bonding into a 3D noninterpenetrated diamond-like network.

4. Conclusion

In conclusion, we have synthesized six Cu(II) complexes with diverse structures by using an asymmetrical aroylhydrazone ligand. The coordinated modes of them altered by simply changing the reaction conditions, leading to the variation from 0D mononuclear to 1D polymer. It is clear that the auxiliary ligands, anions and solvents which can occupy the open coordination sites of Cu(II) and play a crucial role in the molecular structure and supramolecular assembly. Furthermore, the systematic investigation of the influence of reaction conditions on the self-assembly process based on the open coordination sites simultaneously provides a valuable approach for the construction of novel metal-organic complexes with different structures and functional properties.

Acknowledgment

We thank the National Science Council of the People's Republic of China for supporting this research (Nos. 21071018, 21271026).

Appendix A. Supplementary material

Crystallographic data for the structural analysis have been deposited at the Cambridge Crystallographic Data Centre, CCDC No 1052939-1052942, 1052944 and 1052945. These data

can be obtained free of charge via <http://www.ccdc.cam.ac.uk/conts/retrieving.html>, or from the CCDC, 12 Union Road, Cambridge, CB2 1EZ, UK; fax: (+44) 01223-336-033; e-mail: deposit@ccdc.cam.ac.

References

- [1] S. Löffler, J. Lübben, L. Krause, D. Stalke, B. Dittrich, G.H. Clever, Triggered Exchange of Anionic for Neutral Guests inside a Cationic Coordination Cage, *J. Am. Chem. Soc.* 137 (2015) 1060–1063.
- [2] M. Atzori, S. Benmansour, G.M. Espallargas, M. Clemente-León, A. Abhervé, P. Gómez-Claramunt, E. Coronado, F. Artizzu, E. Sessini, P. Deplano, A. Serpe, M.L. Mercuri, C.G. García, A Family of Layered Chiral Porous Magnets Exhibiting Tunable Ordering Temperatures, *Inorg. Chem.* 52 (2013) 10031–10040.
- [3] G. L. Liu, Y. J. Qin, L. Jing, G. Y. Wei, H. Li, Two novel MOF-74 analogs exhibiting unique luminescent selectivity, *Chem. Commun.* 49 (2013) 1699–1701.
- [4] C.Y. Zheng, H. Li, Chirality delivery through multiple and helical H-bonding from chiral coordination complex to its supramolecular architecture, *Inorg. Chem. Commun.* 34 (2013) 30–33.
- [5] B. Mirtamizdoust, B. Shaabani, S.W. Joo, D. Viterbo, G. Croce, Y. Hanifehpour, Sonochemical Synthesis and Structural Characterization and DFT Calculations of a Novel Nano Flower Pb(II) Coordination Compound $[\text{Pb}(\text{phen})_2(4\text{-abs})_2]_n$, *J. Inorg. Organomet. Polym.* 22 (2012) 1397–1403.
- [6] B. Mirtamizdoust, B. Shaabani, A. Khandar, H.-K. Fun, S. Huang, M. Shadman, P. Hojati-Talemi, Direct Synthesis of PbO Nanoparticles From a Lead(II) Nano Coordination Polymer Precursor: Synthesis, Crystal Structure, and DFT Calculations of $[\text{Pb}_2(\text{dmp})_2(\mu\text{-N}_3)_2(\mu\text{-ClO}_4)_2]_n$ with the First $\text{Pb}_2\text{-}(\mu\text{-ClO}_4)_2$ Unit, *Z. Anorg. Allg. Chem.* 638 (2012) 844–850.
- [7] Y. Hanifehpour, B. Mirtamizdoust, S.W. Joo, Synthesis, Structural Investigation and DFT Calculations of Cadmium (II) Fluorine-Substituted β -Diketonate: A Precursor to Producing Pure Phase Nano-Sized Cadmium (II) Oxide, *J. Inorg. Organomet. Polym.* 22 (2012) 816–821.
- [8] B. Mirtamizdoust, S. Ali-Asgari, S.W. Joo, E. Maskani, Y. Hanifehpour, T.H. Oh, New Flower-Shaped Lead(II) Coordination Polymer at the Nano Scale: Synthesis, Structural Characterization and DFT Calculations of $[\text{Pb}(o\text{-phen})(\text{N}_3)_2]_n$ Containing the $\text{Pb}\text{-}(\mu_{1,1}\text{-N}_3)(\mu_{1,3}\text{-N}_3)$ Motif, *J. Inorg. Organomet. Polym.* 23 (2013) 751–757.
- [9] Y. Hanifehpour, A. Morsali, B. Mirtamizdoust, S.W. Joo, Sonochemical synthesis of tri-nuclear lead(II)-azido nano rods coordination polymer with 3,4,7,8-tetramethyl-1,10-phenanthroline (tmph): Crystal structure determination and preparation of nano lead(II) oxide, *J. Mol. Struct.* 1079 (2015) 67–73.
- [10] Y. Hanifehpour, B. Mirtamizdoust, B. Khomami, S.W. Joo, Effects of Halogen Bonding in Chemical Activity of Lead(II) Electron Pair: Sonochemical Synthesis, Structural Studies, and Thermal Analysis of Novel Lead(II) Nano Coordination Polymer, *Z. Anorg. Allg. Chem.* 641 (2015) 2466–2472.
- [11] G.H. Shahverdizadeh, F. Hakimi, B. Mirtamizdoust, A. Soudi, P. Hojati-Talemi, Synthesis

- and Structural Characterization of New Lead(II) Discrete and Infinite Cage-Like Framework: A Precursor to Produce Pure Phase Nano-Sized Lead(II) Oxide, *J. Inorg. Organomet. Polym.* 22 (2012) 903–909.
- [12] Y. Hanifehpour, B. Mirtamizdoust, A. Morsali, S.W. Joo, Sonochemical syntheses of binuclear lead(II)-azido supramolecule with ligand 3,4,7,8-tetramethyl-1,10-phenanthroline as precursor for preparation of lead(II) oxide nanoparticles, *Ultrason. Sonochem.* 23 (2015) 275–281.
- [13] Y. Hanifehpour, V. Safarifard, A. Morsali, B. Mirtamizdoust, S.W. Joo, Sonochemical syntheses of two new flower-like nano-scale high coordinated lead(II) supramolecular coordination polymers, *Ultrason. Sonochem.* 23 (2015) 282–288.
- [14] Y. Hanifehpour, E. Paknahad, B. Mirtamizdoust, S.W. Joo, Solvothermal Synthesis of a Nano-sized Aza-aromatic Base Adduct of a Cadmium(II) 4,4-Difluoro-1-phenyl-1,3-butandionate Coordination Compound, *J. Inorg. Organomet. Polym.* 22 (2012) 1365–1369.
- [15] C.Y. Zheng, R.F. Shi, X. Jin, L. Dong, H. Li, β -Alanine Zn(II) and Cd(II) coordination complexes with diamondoid frameworks possessing second-order nonlinear optics properties, *Inorg. Chem. Commun.* 58 (2015) 74–78.
- [16] K.C. Mondal, A. Sundt, Y.H. Lan, G.E. Kostakis, O. Waldmann, L. Ungur, L.F. Chibotaru, C. E. Anson, A.K. Powell, Coexistence of Distinct Single-Ion and Exchange-Based Mechanisms for Blocking of Magnetization in a $\text{Co}^{\text{II}}_2\text{Dy}^{\text{III}}_2$ Single-Molecule Magnet, *Angew. Chem. Int. Ed.* 51 (2012) 7550–7554.
- [17] M.S. Roodsari, B. Shaabani, B. Mirtamizdoust, M. Dusek, K. Fejfarova, Sonochemical Synthesis of Bismuth(III) Nano Coordination Compound and Direct Synthesis of Bi_2O_3 Nanoparticles from a Bismuth(III) Nano Coordination Compound Precursor, *J. Inorg. Organomet. Polym.* 25 (2015) 1226–1232.
- [18] A.W. Augustyniak, M. Fandzloch, M. Domingo, I. Łakomska, J.A.R. Navarro, A vanadium(IV) pyrazolate metal–organic polyhedron with permanent porosity and adsorption selectivity, *Chem. Commun.* 51 (2015) 14724–14727.
- [19] Y. Hanifehpour, B. Mirtamizdoust, M. Hatami, B. Khomami, S.W. Joo, Synthesis and structural characterization of new bismuth (III) nano coordination polymer: A precursor to produce pure phase nano-sized bismuth (III) oxide, *J. Mol. Struct.* 1091 (2015) 43–48.
- [20] Y. Hanifehpour, B. Mirtamizdoust, S.W. Joo, Sonochemical Synthesis and Characterization of the New Micro-Hexagonal-Rod Lead (II)-Azido Coordination Compound, *J. Inorg. Organomet. Polym.* 22 (2012) 916–922.
- [21] L. Zhang, G.C. Xu, Y. Yang, J.X. Guo, D.Z. Jia, Syntheses, structure diversity and properties of complexes with 4-acyl pyrazolone salicylidene hydrazide derivatives, *Dalton Trans.* 42 (2013) 4248–4257.
- [22] A. Valipour, B. Mirtamizdoust, M. Ghaedi, F. Taghizadeh, P. Talemi, Hemidirected Coordination Sphere on Novel Lead(II) Nano Coordination Polymer: Synthesis, Structural Characterization and DFT Calculation of $[\text{Pb}(\text{p-2-einh})\text{ClO}_4(\text{MeOH})_2]_n$, *J. Inorg. Organomet. Polym.* 26 (2016) 197–207.
- [23] Z. H. Zhang, S. C. Chen, M. Y. He, Q. Chen, M. Du, *Cryst. Growth Des.* 13 (2013) 996–1001.
- [24] Y. Hanifehpour, V. Safarifard, A. Morsali, B. Mirtamizdoust, S.W. Joo, Ultrasound-assisted

- fabrication of a new nano-rods 3D copper(II)-organic coordination supramolecular compound, *Ultrason. Sonochem.* 31 (2016) 201–205.
- [25] H.X. Li, W. Zhao, H.Y. Li, Z.L. Xu, W.X. Wang, J.P. Lang, [Cu₃₀I₁₆(mtpmt)₁₂(μ₁₀-S₄)]: an unusual 30-membered copper(I) cluster derived from the C–S bond cleavage and its use in heterogeneous catalysis, *Chem. Commun.* 49 (2013) 4259–4261.
- [26] M.G. Alexandru, D. Visinescu, M. Andruh, N. Marino, D. Armentano, J. Cano, F. Lloret, M. Julve, Heterotrimetallic Coordination Polymers: {Cu^{II}Ln^{III}Fe^{III}}Chains and {Ni^{II}Ln^{III}Fe^{III}} Layers: Synthesis, Crystal Structures, and Magnetic Properties, *Chem. Eur. J.* 21 (2015) 5429–5446.
- [27] C. He, J. Wang, L. Zhao, T. Liu, J. Zhang, C.Y. Duan, A photoactive basket-like metal–organic tetragon worked as an enzymatic molecular flask for light driven H₂ production, *Chem. Commun.* 49 (2013) 627–629.
- [28] H.J. Zhang, R.Q. Fan, Y.W. Dong, W. Chen, X. Du, P. Wang, Y.L. Yang, Assembly of one-, two-, and three-dimensional Ln(III) complexes constructed from a novel asymmetric tricarboxylic acid: synthesis, structure, photoluminescence and tunable white-light emission, *CrystEngComm.* (2016) DOI: 10.1039/c6ce00483k.
- [29] M. Magott, H. Tomkowiak, A. Katrusiak, W. Nitek, B. Sieklucka, D. Pinkowicz, Two Cyanide-Bridged Mn^{II}–Nb^{IV} Coordination Chain Ferrimagnets Promoted by Interchain Ferromagnetic Interactions, *Inorg. Chem.* (2016) DOI: 10.1021/acs.inorgchem.6b00269.
- [30] D.L. Reger, J. Horger, M.D. Smith, G.J. Long, Homochiral, helical metal–organic framework structures organized by strong, non-covalent π–π stacking interactions, *Chem. Commun.* (2009) 6219–6221.
- [31] J.M. Frost, R.J. Stirling, S. Sanz, N. Vyas, G.S. Nichol, G. Rajaraman, E.K. Brechin, Turning a “useless” ligand into a “useful” ligand: a magneto-structural study of an unusual family of Cu^{II} wheels derived from functionalised phenolic oximes, *Dalton Trans.* 44 (2015) 10177–10187.
- [32] Y.N. Wang, P. Zhang, J.H. Yu, J.Q. Xu, 4-(4-Carboxyphenoxy)phthalate-based coordination polymers and their application in sensing nitrobenzene, *Dalton Trans.* 44 (2015) 1655–1663.
- [33] D. Han, F.L. Jiang, M.Y. Wu, L. Chen, Q.H. Chen, M.C. Hong, A non-interpenetrated porous metal–organic framework with high gas-uptake capacity, *Chem. Commun.* 47 (2011) 9861–9863.
- [34] L.K. Rana, S. Sharma, G. Hundal, First Report on Crystal Engineering of Hg(II) Halides with Fully Substituted 3,4-Pyridinedicarboxamides: Generation of Two-Dimensional Coordination Polymers and Linear Zig-Zag Chains of Mercury Metal Ions, *Cryst. Growth Des.* 16 (2016) 92–107.
- [35] S. Narang, U.P. Singh, P. Venugopalan, Solvent-mediated supramolecular templated assembly of a metal organophosphonate via a crystal–amorphous–crystal transformation, *CrystEngComm.* 18 (2016) 54–61.
- [36] Z.F. Ju, D.Q. Yuan, Wings waving: coordinating solvent-induced structural diversity of new Cu(II) flexible MOFs with crystal to crystal transformation and gas sorption capability, *CrystEngComm.* 15 (2013) 9513–9520.
- [37] H.H. Monfared, M. Vahedpour, M.M. Yeganeh, M. Ghorbanloo, P. Mayer, C. Janiak, Concentration dependent tautomerism in green [Cu(HL¹)(L²)] and brown [Cu(L¹)(HL²)] with H₂L¹ = (E)-N'-(2-hydroxy-3-methoxybenzylidene)benzoylhydrazone and HL² =

- pyridine-4-carboxylic (isonicotinic) acid, Dalton Trans. 40 (2011) 1286–1294.
- [38] W.X. Ni, M. Li, S.Z. Zhan, J.Z. Hou, D. Li, In Situ Immobilization of Metalloligands: A Synthetic Route to Homometallic Mixed-Valence Coordination Polymers, Inorg. Chem. 48 (2009) 1433–1441.
- [39] X.H. Peng, X.L. Tang, W.W. Qin, W. Dou, Y.L. Guo, J.R. Zheng, W.S. Liu, D.Q. Wang, Aroylhydrazone derivative as fluorescent sensor for highly selective recognition of Zn²⁺ ions: syntheses, characterization, crystal structures and spectroscopic properties, Dalton Trans. 40 (2011) 5271–5277.
- [40] D. Matoga, J. Szklarzewicz, R. Gryboś, K. Kurpiewska, W. Nitek, Spacer-Dependent Structural and Physicochemical Diversity in Copper(II) Complexes with Salicyloyl Hydrazones: A Monomer and Soluble Polymers, Inorg. Chem. 50 (2011) 3501–3510.
- [41] A. Ray, C. Rizzoli, G. Pilet, C. Desplanches, E. Garribba, E. Rentschler, S. Mitra, Two New Supramolecular Architectures of Singly Phenoxo-Bridged Copper(II) and Doubly Phenoxo-Bridged Manganese(II) Complexes Derived from an Unusual ONOO Donor Hydrazone Ligand: Syntheses, Structural Variations, Cryomagnetic, DFT, and EPR Studies, Eur. J. Inorg. Chem. (2009) 2915–2928.
- [42] B.B. Tang, X.P. Sun, G.L. Liu, H. Li, Crystal structures of transition metal complexes with an asymmetrical tridentate Schiff-base ligand, J. Mol. Struct. 984 (2010) 111–116.
- [43] K. Das, A. Datta, C. Sinha, J.-H. Huang, E. Garribba, C.-S. Hsiao, C.-L. Hsu, End-to-End Thiocyanato-Bridged Helical Chain Polymer and Dichlorido-Bridged Copper(II) Complexes with a Hydrazone Ligand: Synthesis, Characterisation by Electron Paramagnetic Resonance and Variable-Temperature Magnetic Studies, and Inhibitory Effects on Human Colorectal Carcinoma Cells, ChemistryOpen. 1 (2012) 80–89.
- [44] B.B. Tang, H. Ma, G.Z. Li, Y.B. Wang, G. Anwar, R.F. Shi, H. Li, Synthesis, crystal structures and luminescent properties of tetranuclear Zn molecular clusters with aroylhydrazone ligand, CrystEngComm. 15 (2013) 8069–8073.
- [45] Y.N. Guo, G.F. Xu, W. Wernsdorfer, L. Ungur, Y. Guo, J.K. Tang, H.J. Zhang, L.F. Chibotaru, A.K. Powell, Strong Axiality and Ising Exchange Interaction Suppress Zero-Field Tunneling of Magnetization of an Asymmetric Dy₂ Single-Molecule Magnet, J. Am. Chem. Soc. 133 (2011) 11948–11951.
- [46] P.H. Lin, T.J. Burchell, R. Clérac, M. Murugesu, Dinuclear Dysprosium(III) Single-Molecule Magnets with a Large Anisotropic Barrier, Angew. Chem. Int. Ed. 47 (2008) 8848–8851.
- [47] Y.N. Guo, X.H. Chen, S.F. Xue, J.K. Tang, Modulating Magnetic Dynamics of Three Dy₂ Complexes through Keto–Enol Tautomerism of the *o*-Vanillin Picolinoylhydrazone Ligand, Inorg. Chem. 50 (2011) 9705–9713.
- [48] C.F. Chow, S. Fujii, J.M. Lehn, Metallodynamers: Neutral Dynamic Metallosupramolecular Polymers Displaying Transformation of Mechanical and Optical Properties on Constitutional Exchange, Angew. Chem. 119 (2007) 5095–5098.
- [49] N. Huang, R. Kolhatkar, Y. Eyobo, L. Sorci, I. Rodionova, A.L. Osterman, A.D. MacKerell Jr, H. Zhang, Complexes of Bacterial Nicotinate Mononucleotide Adenylyltransferase with Inhibitors: Implication for Structure-Based Drug Design and Improvement, J. Med. Chem. 53 (2010) 5229–5239.
- [50] D.R. Richardson, D.S. Kalinowski, V. Richardson, P.C. Sharpe, D.B. Lovejoy, M. Islam, P.V. Bernhardt, 2-Acetylpyridine Thiosemicarbazones are Potent Iron Chelators and

- Antiproliferative Agents: Redox Activity, Iron Complexation and Characterization of their Antitumor Activity, *J. Med. Chem.* 52 (2009) 1459–1470.
- [51] C.D. Fan, J. Zhao, B.X. Zhao, S.L. Zhang, J.Y. Miao, Novel Complex of Copper and a Salicylaldehyde Pyrazole Hydrazone Derivative Induces Apoptosis through Up-Regulating Integrin $\beta 4$ in Vascular Endothelial Cells, *Chem. Res. Toxicol.* 22 (2009) 1517–1525.
- [52] D. Sadhukhan, A. Ray, G. Pilet, C. Rizzoli, G.M. Rosair, C.J. Gómez-García, S. Signorella, S. Bellú, S. Mitra, Weak Interactions Modulating the Dimensionality in Supramolecular Architectures in Three New Nickel(II)-Hydrazone Complexes, Magnetostructural Correlation, and Catalytic Potential for Epoxidation of Alkenes under Phase Transfer Conditions, *Inorg. Chem.* 50 (2011) 8326–8339.
- [53] C.L. Wang, W.B. Zhang, C.H. Hsu, H.J. Sun, R.M.V. Horn, Y.F. Tu, D.V. Anokhin, D.A. Ivanov, S.Z.D. Cheng, A supramolecular structure with an alternating arrangement of donors and acceptors constructed by a trans-di-C60-substituted Zn porphyrin derivative in the solid state, *Soft Matter.* 7 (2011) 6135–6143.
- [54] X.L. Ni, X. Xiao, H. Cong, L.L. Liang, K. Cheng, X.J. Cheng, N.N. Ji, Q.J. Zhu, S.F. Xue, Z. Tao, Cucurbit[*n*]uril-based coordination chemistry: from simple coordination complexes to novel poly-dimensional coordination polymers, *Chem. Soc. Rev.* 42 (2013) 9480-9508.
- [55] Y.F. Han, H.Li, G.X. Jin, Host–guest chemistry with bi- and tetra-nuclear macrocyclic metallasupramolecules, *Chem. Commun.* 46 (2010) 6879–6890.
- [56] L. Adriaenssens, P. Ballester, Hydrogen bonded supramolecular capsules with functionalized interiors: the controlled orientation of included guests, *Chem. Soc. Rev.* 42 (2013) 3261–3277.
- [57] G. M. Sheldrick, SHELXS-97, Program for the Refinement of Crystal Structure, University of Göttingen, Germany, 1997.
- [58] Bruker, SMART and SAINT. Bruker AXS Inc., Madison, Wisconsin, USA, 2002.
- [59] G. M. Sheldrick, SADABS. Program for Empirical Absorption Correction of Area Detector, University of Göttingen, Germany, 1996.
- [60] H.H. -Monfared, H. Falakian, R. Bikas, P. Mayer, Intramolecular hydrogen bond effect on keto-enolization of aroylhydrazone in copper(II) complexes, *Inorg. Chim. Acta.* 394 (2013) 526–534.
- [61] A.W. Addison, T.N. Rao, J. Reedijk, J. Rijn, G.C. Verschoor, Synthesis, Structure, and Spectroscopic Properties of Copper(II) Compounds containing Nitrogen-Sulphur Donor Ligands; the Crystal and Molecular Structure of Aqua [1,7-bis(N-methylbenzimidazol-2'-yl)-2,6-dithiaheptane] copper(II) Perchlorate, *J. Chem. Soc. Dalton Trans.* (1984) 1349–1356.
- [62] S. Roy, P. Mitra, A.K. Patra, Cu(II) complexes with square pyramidal (N₂S)CuCl₂ chromophore: Jahn–Teller distortion and subsequent effect on spectral and structural properties, *Inorg. Chim. Acta.* 370 (2011) 247–253.
- [63] V. Sahe, I. Sheikshoae, N. Setoodeh, H.A. Rudbari, G. Bruno, A new tridentate Schiff base Cu(II) complex: Synthesis, experimental and theoretical studies on its crystal structure, FT-IR and UV–Visible spectra *Spectrochim. Acta A Mol Biomol Spectrosc.* 110 (2013) 124–129.

- 1 Six Cu(II) complexes containing asymmetrical aroylhydrazone ligand were synthesized and analyzed by x-ray single crystal diffraction.
- 2 By controlling the synthetic conditions and guest species, an effective way to create the open coordination sites in coordination complexes was offered.
- 3 Hydrogen bonds exist in all six complexes to construct supramolecular architecture.